

ABSTRACT

10 The LATEX (LAgrangian Transport EXperiment) project was developed to study the
11 influence of coupled physical and biogeochemical dynamics at the meso- and submeso-scale
12 on the transfers of matter and heat between the coastal zone and the open ocean. One of the
13 goals of the Latex10 field experiment, conducted during September 2010 in the Gulf of Lion
14 (NW Mediterranean), was to mark a dynamical mesoscale feature by releasing a passive
15 tracer (Sulfur Hexafluoride-SF₆) together with an array of Lagrangian buoys. The goal
16 was to release the tracer in an initial patch as homogeneous as possible in the horizontal,
17 and to study its turbulent mixing and dispersion while minimizing the contribution due
18 to the advection. For that, it was necessary to continuously adjust the vessel route in
19 order to remain as closely as possible in the Lagrangian reference frame moving with the
20 investigated mesoscale structure. To accomplish this task, we developed the methodology
21 and the software presented here. The software is equipped with a series of graphical and
22 user-friendly accessories and the entire package for Matlab can be freely downloaded from
23 <http://mio.pytheas.univ-amu.fr/~doglioli> .

24 1. Introduction

25 The importance of a Lagrangian sampling strategy for the analysis of tracer dispersion has
26 been evidenced by pioneer studies within the IronEx project, the first in situ iron-enrichment
27 experiment (Law et al. 1998; Stanton et al. 1998). In fact, only the measurements collected
28 in a Lagrangian reference frame moving with a tracer patch allow to correct the tracer
29 budget for the effect due to water advection, and thus permit its accurate estimation. The
30 Lagrangian-based navigation system developed for the IronEx experiment has been briefly
31 described by Coale et al. (1998). Their system was used during the tracer release to correct
32 the ship route with respect to the current drift in order to introduce in the environment an
33 initial patch as square as possible in the horizontal. The center of the Lagrangian reference
34 frame was defined by the position of a drogued buoy deployed before the tracer release. The
35 buoy was equipped with a Global Positioning System (GPS) receiver connected to a very
36 high frequency (VHF) packet radio transmitter. Onboard a VHF receiver was interfaced
37 with a computer. A specific software was developed in order to display the ship and buoy
38 positions overlaid to the injection (or sampling) grid.

39 Release and tracking of a tracer patch within a Lagrangian reference frame was also at
40 the base of the PRIME project (Law et al. 2001). During the field experiment an eddy
41 was marked with ARGOS buoys and a passive tracer (Sulfur Hexafluoride-SF₆) was released
42 in a Lagrangian framework using a dead-reckoning strategy. Such strategy included cor-
43 rections for surface-water advection: the projected ship trajectory was adjusted according
44 to the ship-recorded surface current measurements in order to release the tracer following
45 the same water mass. One major disadvantage of dead-reckoning is that, between successive
46 known positions, or fixes, the ship trajectory adjustments are estimated using only previously
47 recorded information, kept constant in time. Errors and uncertainties are thus cumulative
48 and tend to grow with time, limiting the accuracy of such strategy. Hence, subsequent in
49 situ Lagrangian addition experiments, such as SOIREE (Boyd and Law 2001), CYCLOPS
50 (Law et al. 2005), SEEDS (Tsumune et al. 2005) and SEEDS II (Tsumune et al. 2009),

51 were all performed adopting the older technique first developed for the IronEX project (Law
52 et al. 1998). Minor modifications to this strategy were then implemented within the SERIES
53 experiment (Law et al. 2006), during which the Lagrangian tracer release was coordinated
54 using the ECPINS[©] package. This is a commercial search and rescue computerized package
55 for shipboard navigational aid that displays electronic charts and the ship's position in real
56 time along with sensor data¹. To our knowledge, no other papers report detailed descriptions
57 of the techniques and software adopted for Lagrangian tracer release and sampling strategy,
58 although they are a key point for the success of in situ tracer experiments.

59 In this article we will describe the methodological approach and the technological ad-
60 vances (hardware and software) developed during the LATEX project (LAgrangian Trans-
61 port EXperiment, 2008-2010; <http://www.com.univ-mrs.fr/LOPB/LATEX>). LATEX was
62 designed to study the influence of the coupled physical and biogeochemical dynamics at the
63 meso- and submeso-scales on the transfers of matter and heat between the coastal zone and
64 the open ocean. In order to reach this goal, the project was highly multidisciplinary, with
65 a strategy based on a combined use of satellite data, numerical model results and in situ
66 measurements from a series of four field campaigns. The main goal of the field experiment
67 was to analyze transport patterns and dispersion rates of a mesoscale structure within the
68 Lagrangian reference frame associated with it. Therefore, the experiment was designed to
69 combine the release of SF6 with the deployment of an array of Lagrangian buoys. Two of
70 the four LATEX's field campaigns were dedicated to the tracer release experiment. The first
71 one, the Latex00 campaign (9-11 June 2007), was part of a pilot project which aimed to
72 demonstrate the feasibility of our methodology. During the last one, the Latex10 campaign
73 (1-24 September 2010), we first tested, and then succesfully performed, the tracer release.
74 The LATEX's field campaigns were conducted in the Gulf of Lion (Fig. 1). This region is
75 particularly appropriate for studying coastal mesoscale dynamics and its role in cross-shelf
76 exchanges. In fact, exchanges between the Gulf of Lion and offshore waters are mainly

¹http://osigeospatial.com/offshoresystems/pdf/OSI_ECPINS-5000.pdf

77 induced by processes associated with the the Northern Current (Conan and Millot 1995;
78 Flexas et al. 2002; Petrenko et al. 2005). The Northern Current is an alongslope density
79 current that exhibits an important mesoscale activity induced by i) topographical forcing;
80 ii) interaction with the strong northely and north-westerly winds (Mistral and Tramontane),
81 and iii) presence of the Rhône river freshwater discharge (e.g. Schaeffer et al. 2011, and
82 references therein).

83 On the basis of a 10-years realistic simulation from a high-resolution numerical model
84 (Hu et al. 2009, 2011a; Campbell et al. 2013), the western part of the Gulf of Lion was
85 choosen to be investigated by two exploratory campaings, Latex08 (1-5 September 2008)
86 and Latex09 (24-28 August 2009). The results of both campaings evidenced the presence
87 of anticyclonic eddies at the end of the summer (Hu et al. 2011b; Kersalé et al. 2013). For
88 this reason, the Latex10 cruise was organized in the same region during the same period of
89 the year. Finally, the area for the tracer dispersion experiment was selected combining the
90 numerical model results with the results from near-realtime analysis of Finite Size Lyapunov
91 Exponents computed from both satellite-altimetry derived currents and iterative releases of
92 subsurface drifters (Nencioli et al. 2011).

93 Our Lagrangian strategy presents some important technological improvements with re-
94 spect to previous tracer studies. In this paper we intend to evidence the advancements lead-
95 ing to an increased accuracy in the Lagrangian navigation. Futhermore, we also announce
96 the first release of a dedicated free software package for the application of our methodology.

97 2. Background

98 The budget of a given tracer can be described by the continuity equation for its concen-
99 tration ψ expressed as:

$$100 \quad \frac{d}{dt} \int_V \psi dV + \oint_S \psi \mathbf{v} \cdot d\mathbf{S} + \oint_S \chi \cdot d\mathbf{S} + \int_V \xi dV = 0 \quad (1)$$

101 The temporal variation of ψ in the volume V (first term) is balanced by the variations across
102 the volume surface S due to the advection by the current field \mathbf{v} (second term) and to other
103 surface exchanges χ (third term), and by the sources and sinks ξ within the volume V (fourth
104 term). Using a Lagrangian reference frame to investigate a tracer budget is particularly
105 advantageous since the second term of Eq. (1) becomes null. Moreover, if the budget is
106 derived for a conservative tracer as the SF6, the fourth term also becomes null. Thus, when
107 the two conditions above are fulfilled, it becomes possible to estimate the exchanges χ by
108 measuring the temporal variation only. In the ocean, for dissolved material or particles
109 small enough to have negligible settling velocity, such exchanges χ are the fluxes due to
110 the vertical and horizontal turbulent mixing (e.g. Hillmer and Imberger 2007, for the case of
111 a cylindrical volume). Being properties of the flow, χ can be considered identical for both
112 conservative and non-conservative tracers. Therefore, by using a Lagrangian reference frame
113 and retrieving the turbulent fluxes from the budget of a conservative tracer, it is possible
114 to estimate the sources and sinks of other non-conservative (i.e. biogeochemical) tracers by
115 simultaneously measuring their temporal variation.

116 The approach described above has been adopted during the Latex10 cruise. A key aspect
117 of the in situ experiment has been to plan in real-time the ship route in the Lagrangian refer-
118 ence frame for the release of the conservative tracer and the successive samplings. Generally,
119 a route is characterized by a number of “turn points”, which are the positions at which a
120 new direction is taken to reach the following turn point. In a Lagrangian reference frame
121 the position of each turn point moves with the water mass under investigation. Thus, it
122 is necessary to continuously adjust the ship route towards the moving turn points. This is
123 achieved using a classical ballistic approach under the following assumptions:

- 124 i. ship speed is constant and faster than the buoy speed;
- 125 ii. there is no stirring and no rotation associated with the investigated water mass.

126 The first assumption can easily be respected during a field experiment with a modern re-

127 search vessel. Some attention has just to be given to the design of the tracer release system
128 in order to allow a release rate fast enough not to pose limitations to the ship speed in
129 case the experiment is planned in very energetic regions. Whereas, the second assumption
130 may appear severe. However, unlike advection, stirring and rotation can be considered slow
131 processes with respect to the tracer release or sampling. Estimating stirring and rotation
132 would be possible by releasing at sea a large number of buoys, but it would significantly
133 increase the cruise costs. We numerically tested the validity of such an assumption with a
134 simple Lagrangian random-walk model. By using an idealized current fields we performed
135 several comparisons on the resulting concentrations with and without stirring and rotation.
136 Our numerical results confirmed the validity of this second assumption². Therefore, in the
137 present work, just as in previous tracers experiments at sea, we also adopted it.

138 Defining :

- 139 i. $\mathbf{v}_{vessel} \equiv (u_{vessel}, v_{vessel})$ as the vessel speed. Its modulus during LATEX experiments
140 was kept as constant as possible (in our case 3 knots for technical reasons associated
141 to the SF6 release system);
- 142 ii. $\mathbf{v}_{target} \equiv (u_{target}, v_{target})$ as the drift speed of a turn point (x_{target}, y_{target}) of the route.
143 It is assumed to be equal to the drift speed of a buoy released at the point of departure
144 to mark the center of the water mass. This buoy (hereinafter reference buoy) represents
145 the moving origin of the Lagrangian reference frame;

146 we need to solve the following closed equation system:

$$\begin{aligned}
147 \quad x_{vessel} + u_{vessel} t &= x_{target} + u_{target} t \\
148 \quad y_{vessel} + v_{vessel} t &= y_{target} + v_{target} t \\
149 \quad u_{vessel}^2 + v_{vessel}^2 &= |\mathbf{v}_{vessel}|^2
\end{aligned} \tag{2}$$

150 The above system can be reduced to the following quadratic equation in time:

$$151 \quad a t^2 + b t + c = 0 \tag{3}$$

²Data not shown. The testing algorithm is part of the free software package available online.

152 where

$$\begin{aligned}
153 \quad a &= u_{target}^2 + v_{target}^2 - |\mathbf{v}_{vessel}|^2 \\
154 \quad b &= 2[(x_{target} - x_{vessel}) u_{target} + (y_{target} - y_{vessel}) v_{target}] \\
155 \quad c &= (x_{target} - x_{vessel})^2 + (y_{target} - y_{vessel})^2
\end{aligned}$$

156 Excluding the trivial case in which vessel and buoy are both at rest and positioned at the
157 same point, the discriminant of Eq. (3) is always strictly positive. In fact, $c > 0$ and,
158 under the above-mentioned second assumption (vessel speed faster than buoy speed), $a < 0$.
159 Therefore, in case of practical oceanographic applications, Eq. (3) admits two real solutions
160 which are always of opposite sign. The time required for the vessel to reach the target \hat{t} is
161 thus the positive solution. With \hat{t} , we can estimate the updated vessel velocity $(\hat{u}_{vessel}, \hat{v}_{vessel})$
162 as

$$\begin{aligned}
163 \quad \hat{u}_{vessel} &= \frac{(x_{target} - x_{vessel})}{\hat{t}} + u_{target} \\
164 \quad \hat{v}_{vessel} &= \frac{(y_{target} - y_{vessel})}{\hat{t}} + v_{target}
\end{aligned}$$

165 which, in turn, provides the distance between the vessel and the turn point

$$166 \quad \hat{d} = \sqrt{(\hat{u}_{vessel})^2 + (\hat{v}_{vessel})^2} \hat{t}.$$

167 and the updated direction of the vessel (angle $\hat{\alpha}$ in relation to the North) that takes into
168 account the drift of the water mass

$$169 \quad \hat{\alpha} = \begin{cases} 90^\circ - \arctan(\hat{v}_{vessel}/\hat{u}_{vessel}) & \text{for } \hat{u}_{vessel} > 0, \\ 180^\circ & \text{for } \hat{u}_{vessel} = 0 \text{ and } \hat{v}_{vessel} < 0, \\ 0^\circ & \text{for } \hat{u}_{vessel} = 0 \text{ and } \hat{v}_{vessel} > 0, \\ 270^\circ - \arctan(\hat{v}_{vessel}/\hat{u}_{vessel}) & \text{for } \hat{u}_{vessel} < 0, \end{cases}$$

170 with $\arctan(\hat{v}_{vessel}/\hat{u}_{vessel}) \in (-90^\circ, +90^\circ)$.

171 In the rare case that both $\hat{u}_{vessel} = 0$ and $\hat{v}_{vessel} = 0$, the previous direction is maintained.

3. Technological development and field experience

To apply the strategy described in the previous section, we developed a software which solves the equation system (2) and provides in real-time the direction $\hat{\alpha}$ and the distance \hat{d} through a user-friendly graphical interface. The scientist in charge of the Lagrangian navigation can then communicate this information to the bridge to update the ship route.

One of the key aspects for the implementation of the software consists in knowing, in due time, both the position of the vessel and that of the reference buoy. The vessel position can be easily acquired at very high frequency from the onboard positioning system. On the other hand, the reference buoy position needs to be transmitted onboard. Three different transmission systems between the ship and the reference buoy have been considered: HF/VHF radio, Argos and Iridium.

The HF/VHF solution has been excluded, since, despite its potential long-range performance, the required large size of the antenna mounted on the buoy would have influenced its drifting. Indeed, during IronEx, Coale et al. (1998) reported that the buoy extended about 2 m above sea level and, thus, a daily correction based on the tracer concentration itself had to be applied for wind and current effects (Stanton et al. 1998).

The Argos solution has been adopted for the first tests at sea during Latex00 cruise offshore of Marseille (Fig. 1). Our setup included a receiver board Martec RMD03 and an external antenna in order to allow direct communication between the reference buoy and the vessel. In fact, the standard Argos satellite communication would not have provided the reference buoy positions rapidly enough, due to the system procedure for data processing and transmission. Although a range of five miles was expected, it was only possible to obtain a communication range of one mile. This was probably due to the fact that the receiver, despite being positioned as high as possible on the mast, was only 10 meters above sea level. Such range would have posed a strong limitation to the extension of the conservative tracer release and samplings. Thus, the Argos transmission system was rejected for the following field campaigns. Nonetheless, this configuration allowed us to test the software

199 development and to validate the method. In particular, during Latex00, we tested the
200 software by performing two routes of different shapes: a radiator and an expanding square
201 spiral. The radiator is the route shape most frequently cited in literature. It was adopted
202 during the IronEX (Coale et al. 1998), PRIME (Law et al. 2001), SEEDS and SEEDS II
203 (Tsumune et al. 2005, 2009) experiments. The expanding square spiral was instead adopted
204 during the SERIES experiment (Law et al. 2006). During the SOIREE (Boyd and Law 2001)
205 and CYCLOPS (Law et al. 2005) experiments, an expanding hexagon route was also used,
206 but we considered such shape too complex. In fact, with respect to the expanding square
207 spiral, the expanding hexagon route has 50% more turn points (6 instead of 4 for every cycle)
208 without any theoretical advantage. As an example, the Lagrangian-corrected route presented
209 by Law et al. (2005) in their Fig.1C appears very irregular.

210 During the first test of Latex00 (radiator route), the drift of the reference buoy, equipped
211 with a 6m long holey-sock drogue centered at 15-m depth, was essentially northwestward,
212 with a velocity of the order of 0.1 ms^{-1} (Fig. 2a). The Lagrangian corrected ship track
213 shows a good agreement with respect to the expected route. Nevertheless, we observed large
214 discrepancies at most turn points (Fig. 2b). Indeed, the Argos time interval of communication
215 was still quite large (about 15 minutes). Therefore, it did not provide sufficient information
216 nearby the turn points to supply the new ship direction in due time.

217 During the second test of Latex00 (expanding square spiral route), the software worked
218 quite well, although uncertainties appeared again nearby the turn points (Fig. 3). Neverthe-
219 less, this latter shape turned out to be easier to follow due to the increasing time interval
220 between successive turn points. Another advantage is that the route can begin at the deploy-
221 ment position of the reference buoy. Hence, the expanding square spiral route was chosen
222 for the Latex10 cruise.

223 The signal range and communication delay problems of the Argos system described above
224 led us to take into consideration the Iridium transmission system. The Iridium network cov-
225 ers the whole Earth thanks to a satellite constellation mainly used for hand-held phone com-

226 munications. In 2007, at the beginning of our project some manufacturers were beginning
227 to develop Iridium buoys. Indeed, MetOcean provided Iridium SVP Drifters. Nevertheless,
228 the MetOcean buoys i) sent data once per hour, ii) the transmission frequency was not ad-
229 justable, iii) there was no receiver to receive messages directly on board and iv) there was
230 no possibility to remotely change the buoy setup. Therefore, we decided to develop our own
231 prototype buoy with an Iridium transmitter/receiver (Fig. 4). This system was developed by
232 *e-Track*³ and consists in a bi-directional satellite telephone system, which allows for world-
233 wide communication and transmits data as SBD (Short Burst Data, somewhat equivalent
234 to the Short Message System of mobile phones). The SBD are transmitted via satellite from
235 the buoy to an on-shore station, that, in turn, transfers the information via satellite to the
236 vessel. The time interval between the buoy emission and the on-board reception is certified
237 to be less than 1 minute in 99% of the cases. This way, we obtained a buoy extremely com-
238 pact with a worldwide range of transmission and a frequency of communication practically
239 limited only by cost and/or battery life.

240 This system has been used during the Latex10 cruise. We equipped the prototype buoy
241 with a 6m long holey-sock drogue centered at 11.5-m depth. Before the tracer release, we
242 performed a 6-hour test, during which the reference buoy moved initially southward, then
243 westward (Fig. 5a). The Iridium communication worked well and the delay problems at turn
244 points were greatly reduced (Fig. 5b). Nevertheless, thanks to the higher precision obtained,
245 we identified a bug in the code, generating a northwestward shift of the route with respect
246 the theoretical spiral. We were able to rapidly fix it.

247 Finally, during the SF6 release, the software worked very well. Although the reference
248 buoy followed a more complicate trajectory than the previous tests (Fig. 6a), the Lagrangian
249 corrected ship track was in very good agreement with the expected route (Fig. 6b). The
250 initial deviation from the expected spiral is only due to the ship drift during the setup of the

³The e-Track brand, now part of NSE Industries, is specialized in tracking solutions and data transmission;
<http://e-track.ect-industries.fr>.

251 SF6 release device after the deployment of the reference buoy, while the second turn around
252 the last spiral branch is due to the deployment of several Argos buoys around the SF6 patch.

253 4. Concluding remarks

254 This paper intends to present a method to perform vessel routes in a Lagrangian reference
255 frame for in situ tracer experiments. With respect to previous works, we describe in details
256 our theoretical approach based on a simple system of ballistic equations. Moreover, we report
257 the tests we performed on different communication systems between the buoy marking the
258 water mass and the research vessel. Such tests lead to the development of a prototype buoy
259 with bi-directional worldwide-range Iridium communication system. The software developed
260 to manage the Lagrangian navigation worked very well during Latex10 cruise and allowed
261 to release the passive tracer in a square patch very precisely. Such a software is equipped
262 with a series of graphical and user-friendly accessories for i) planning in near-real time the
263 vessel route and sampling stations; ii) treating and mapping oceanographic cruise data; iii)
264 simulating tracer injection and dispersion in idealized conditions by a Lagrangian single
265 particle numerical model. The entire package for Matlab is distributed in the hope that
266 it will be useful for the oceanographic community and it can be freely downloaded from
267 <http://mio.pytheas.univ-amu.fr/~doglioli>.

268 Future foreseeable developments include the possibility to take more advantage of the
269 bidirectional Iridium communication, by implementing an automatic position query to the
270 reference buoy when the vessel is nearby turn points. Moreover, as already mentioned in
271 section 2, multi-buoy marking of the water mass could also be considered for i) a more precise
272 positioning of the center of the Lagrangian reference frame and ii) an estimation of rotation
273 and stirring effects of the investigated water mass.

274 *Acknowledgments.*

275 The LATEX project is supported by the programs LEFE/IDAO and LEFE/CYBER of
276 the CNRS/INSU and by the Region PACA. We thank the crews of the *R/V Le Suroît* and
277 the *R/V Téthys II* and all the LATEX collaborators.

REFERENCES

- 280 Boyd, P. and C. Law, 2001: The Southern Ocean Iron RElease Experiment (SOIREE)
281 - introduction and summary. *Deep-Sea Res. II*, **48 (1112)**, 2425 – 2438, doi:10.1016/
282 S0967-0645(01)00002-9.
- 283 Campbell, R., F. Diaz, Z. Hu, A. Doglioli, A. Petrenko, and I. Dekeyser, 2013: Nutrients
284 and plankton spatial distributions induced by a coastal eddy in the Gulf of Lion. Insights
285 from a numerical model. *Prog. Oceanogr.*, **109**, 47 – 69, doi:10.1016/j.pocean.2012.09.005.
- 286 Coale, K. H., K. S. Johnson, S. E. Fitzwater, S. P. Blain, T. P. Stanton, and T. L. Coley, 1998:
287 IronEx-I, an in situ iron-enrichment experiment: Experimental design, implementation
288 and results. *Deep-Sea Res. II*, **45 (6)**, 919 – 945, doi:10.1016/S0967-0645(98)00019-8.
- 289 Conan, P. and C. Millot, 1995: Variability of the Northern Current off Marseilles, western
290 Mediterranean Sea, from February to June 1992. *Oceanol. Acta*, **182**, 193–205.
- 291 Flexas, M. M., X. Durrieu de Madron, M. A. Garcia, M. Canals, and P. Arnau, 2002: Flow
292 variability in the Gulf of Lions during the MATER HFF experiment (March-May 1997).
293 *J. Mar. Sys.*, **33-34**, 197 – 214, doi:10.1016/S0924-7963(02)00059-3.
- 294 Hillmer, I. and J. Imberger, 2007: Estimating in situ phytoplankton growth rates with a
295 Lagrangian sampling strategy. *Limnol. Oceanogr.-Meth.*, **5**, 495 – 509.
- 296 Hu, Z. Y., A. A. Doglioli, A. M. Petrenko, P. Marsaleix, and I. Dekeyser, 2009: Numerical
297 simulations of eddies in the Gulf of Lion. *Ocean Model.*, **28 (4)**, 203 – 208, doi:10.1016/j.
298 ocemod.2009.02.004.
- 299 Hu, Z. Y., A. A. Petrenko, A. M. Doglioli, and I. Dekeyser, 2011a: Numerical study of

300 eddy generation in the western part of the Gulf of Lion. *J. Geophys. Res.*, **116**, 12030,
301 doi:10.1029/2011JC007074.

302 Hu, Z. Y., A. A. Petrenko, A. M. Doglioli, and I. Dekeyser, 2011b: Study of a mesoscale
303 anticyclonic eddy in the western part of the Gulf of Lion. *J. Mar. Sys.*, **88**, 3–11, doi:
304 10.1016/j.jmarsys.2011.02.008.

305 Kersalé, M., A. A. Petrenko, A. M. Doglioli, I. Dekeyser, and F. Nencioli, 2013: Physical
306 characteristics and dynamics of the coastal Latex09 Eddy derived from in situ data and
307 numerical modeling. *J. Geophys. Res.*, **118**, 399–409, doi:10.1029/2012JC008229.

308 Law, C., E. Abraham, E. Woodward, M. Liddicoat, T. Fileman, T. Thingstad, V. Kitidis,
309 and T. Zohary, 2005: The fate of phosphate in an in situ Lagrangian addition experiment
310 in the Eastern Mediterranean. *Deep-Sea Res. II*, **52 (2223)**, 2911 – 2927, doi:10.1016/j.
311 dsr2.2005.08.017.

312 Law, C., A. Martin, M. Liddicoat, A. Watson, K. Richards, and E. Woodward, 2001: A La-
313 grangian SF_6 tracer study of an anticyclonic eddy in the North Atlantic: patch evolution,
314 vertical mixing and nutrient supply to the mixed layer. *Deep-Sea Res. II*, **48**, 705–724.

315 Law, C., A. Watson, M. Liddicoat, and T. Stanton, 1998: Sulphur hexafluoride as a tracer
316 of biogeochemical and physical processes in an open-ocean iron fertilisation experiment.
317 *Deep-Sea Res. II*, **45 (6)**, 977 – 994, doi:10.1016/S0967-0645(98)00022-8.

318 Law, C. S., et al., 2006: Patch evolution and the biogeochemical impact of entrainment
319 during an iron fertilisation experiment in the subArctic Pacific. *Deep-Sea Res. II*, **53**,
320 2012–2033, doi:10.1016/j.dsr2.2006.05.028.

321 Nencioli, F., F. d’Ovidio, A. M. Doglioli, and A. A. Petrenko, 2011: Surface coastal circula-
322 tion patterns by in-situ detection of Lagrangian coherent structures. *Geophys. Res. Lett.*,
323 **38**, 17604, doi:10.1029/2011GL048815.

- 324 Petrenko, A. A., Y. Leredde, and P. Marsaleix, 2005: Circulation in a stratified and wind-
325 forced Gulf of Lions, NW Mediterranean Sea: *in situ* and modeling data. *Cont. Shelf Res.*,
326 **25**, 7–27, doi:10.1016/j.csr.2004.09.004.
- 327 Schaeffer, A., A. Molcard, P. Forget, P. Fraunié, and P. Garreau, 2011: Generation mecha-
328 nisms for mesoscale eddies in the Gulf of Lions: radar observation and modeling. *Ocean Dy-*
329 *nam.*, **61**, 1587–1609, doi:10.1007/s10236-011-0482-8.
- 330 Stanton, T., C. Law, and A. Watson, 1998: Physical evolution of the IronEx-I open ocean
331 tracer patch. *Deep-Sea Res. II*, **45 (6)**, 947 – 975, doi:10.1016/S0967-0645(98)00018-6.
- 332 Tsumune, D., J. Nishioka, A. Shimamoto, S. Takeda, and A. Tsuda, 2005: Physical behavior
333 of the SEEDS iron-fertilized patch by sulphur hexafluoride tracer release. *Prog. Oceanogr.*,
334 **64 (24)**, 111 – 127, doi:10.1016/j.pocean.2005.02.018.
- 335 Tsumune, D., et al., 2009: Physical behaviors of the iron-fertilized patch in SEEDS II.
336 *Deep-Sea Res. II*, **56 (26)**, 2948 – 2957, doi:10.1016/j.dsr2.2009.07.004.

337 List of Figures

- 338 1 Bathymetry of the Gulf of Lion (isobaths 100, 200 and 1000 m). The arrows
339 represent the Northern Current, the Mistral and Tramontane winds and the
340 Rhône river freshwater discharge. The dot-dashed (dashed) circle shows the
341 area of the Latex10 (Latex00) cruise. The black square shows the tracer
342 release area. 17
- 343 2 The radiator test during the Latex00 cruise. a) Vessel (black) and buoy (gray)
344 tracks in geographical coordinates. The tracking of the ship route begins
345 at the time of deployment of the reference buoy. b) Expected (gray) and
346 obtained (black) vessel tracks in the Lagrangian reference frame. The end of
347 the ship route is indicated in the bottom panel. The first part of the ship
348 route corresponds to the vessel repositioning from the point of deployment of
349 the reference buoy to the beginning of the radiator shape. Large discrepancies
350 are observed at most turn points, in particular at (-0.2,-1.6) and (0.8,-1.6). 18
- 351 3 Same as Fig. 2, but for the expanding square spiral test during the Latex00
352 cruise. Discrepancies are again observed nearby turn points (-0.5,0.5), (0.5,-
353 0.5), (1,1) and (1.5,1.5). 19
- 354 4 Pictures of the prototype buoy. a) The Iridium transmitter/receiver inside
355 the buoy. b) Recovery of the buoy during the Latex10 cruise. The lifeline and
356 the small float were added to facilitate deployment and recovery operations. 20
- 357 5 Same as Fig. 2, but for the 6-hour test during the Latex10 cruise. The NW
358 shift of the Lagrangian corrected route was due to a bug in the first version
359 of the code (see text). 21
- 360 6 Same as Fig. 2, but for the tracer release during the Latex10 cruise. 22

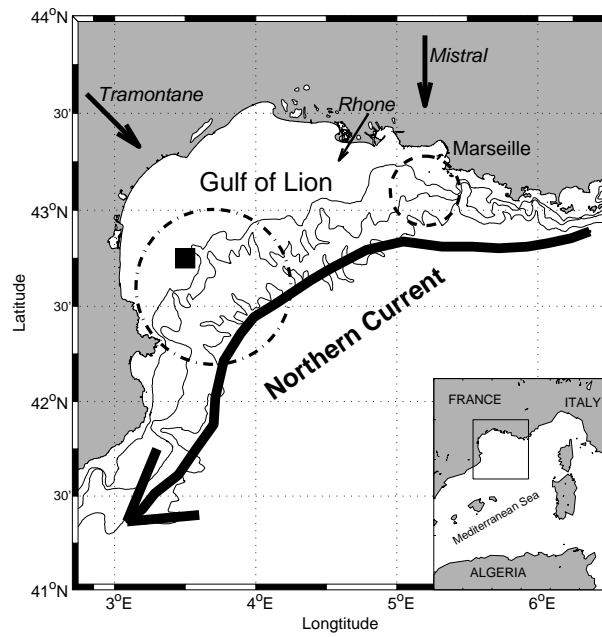


FIG. 1. Bathymetry of the Gulf of Lion (isobaths 100, 200 and 1000 m). The arrows represent the Northern Current, the Mistral and Tramontane winds and the Rhône river freshwater discharge. The dot-dashed (dashed) circle shows the area of the Latex10 (Latex00) cruise. The black square shows the tracer release area.

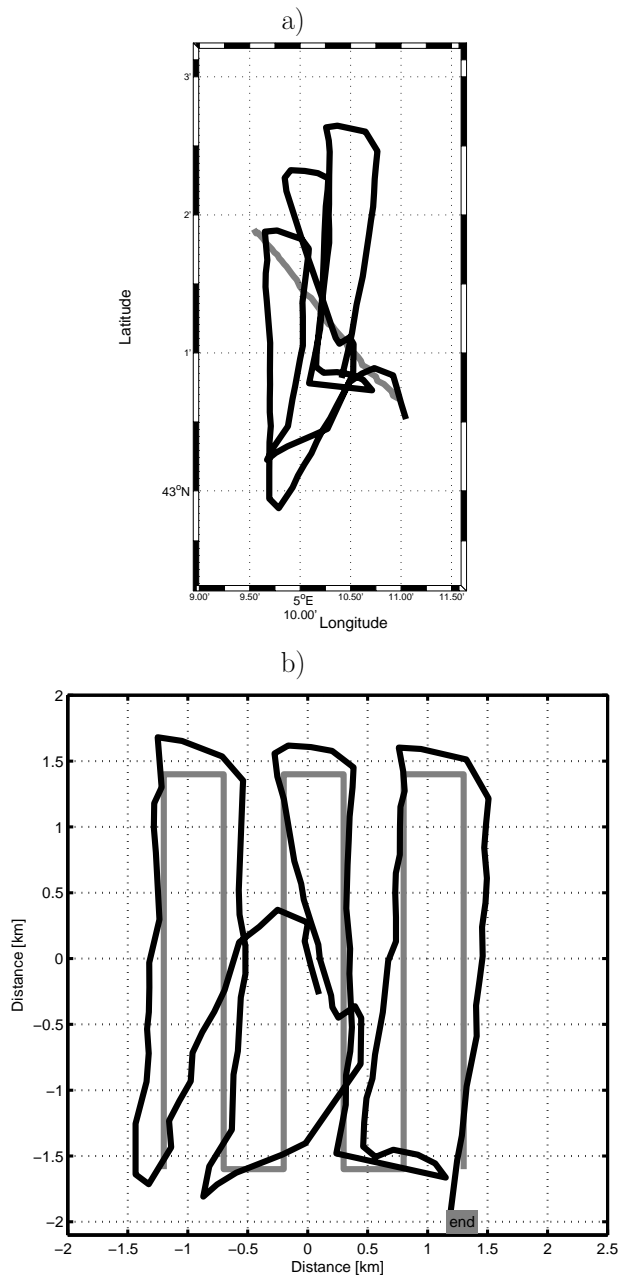


FIG. 2. The radiator test during the Latex00 cruise. a) Vessel (black) and buoy (gray) tracks in geographical coordinates. The tracking of the ship route begins at the time of deployment of the reference buoy. b) Expected (gray) and obtained (black) vessel tracks in the Lagrangian reference frame. The end of the ship route is indicated in the bottom panel. The first part of the ship route corresponds to the vessel repositioning from the point of deployment of the reference buoy to the beginning of the radiator shape. Large discrepancies are observed at most turn points, in particular at $(-0.2, -1.6)$ and $(0.8, -1.6)$.

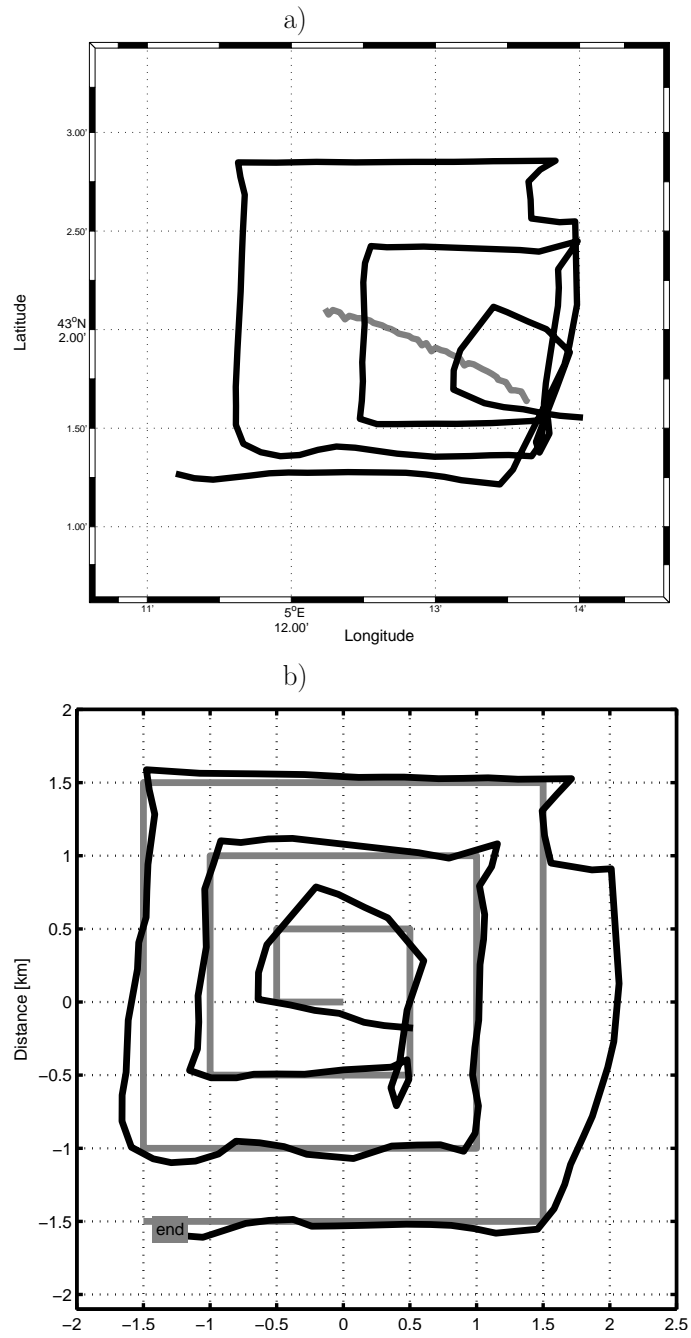


FIG. 3. Same as Fig. 2, but for the expanding square spiral test during the Latex00 cruise. Discrepancies are again observed nearby turn points $(-0.5, 0.5)$, $(0.5, -0.5)$, $(1, 1)$ and $(1.5, 1.5)$.

a)



b)



FIG. 4. Pictures of the prototype buoy. a) The Iridium transmitter/receiver inside the buoy. b) Recovery of the buoy during the Latex10 cruise. The lifeline and the small float were added to facilitate deployment and recovery operations.

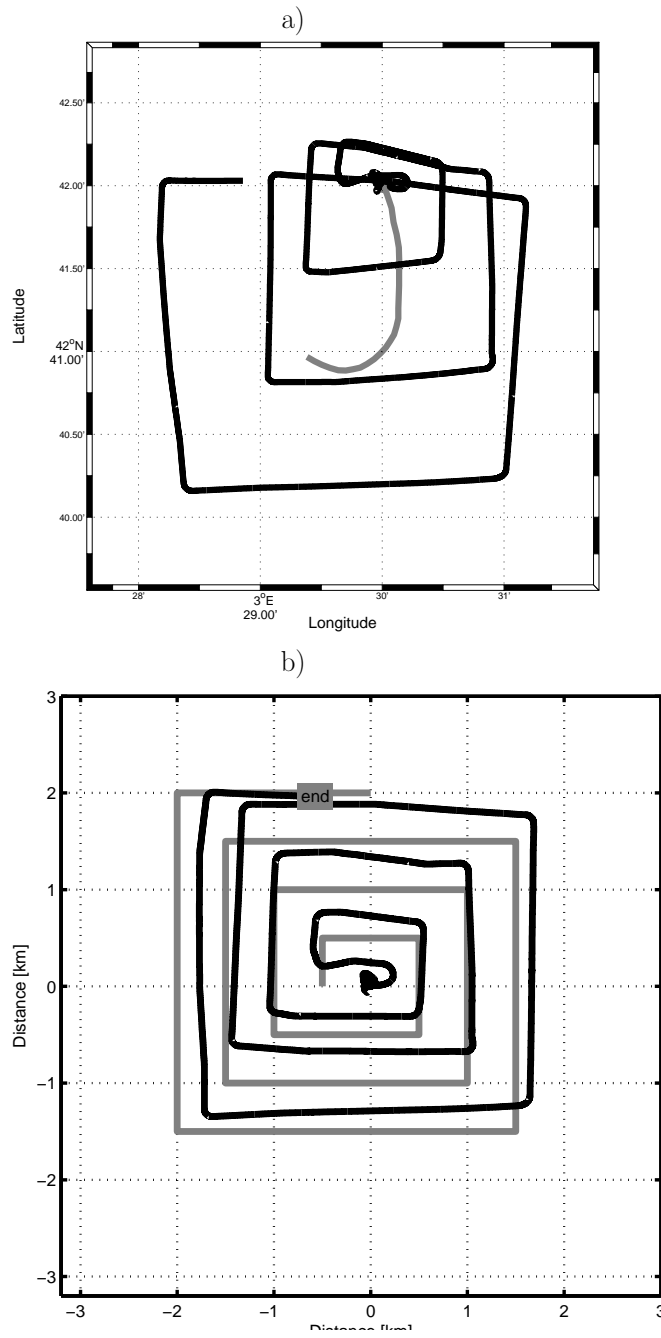


FIG. 5. Same as Fig. 2, but for the 6-hour test during the Latex10 cruise. The NW shift of the Lagrangian corrected route was due to a bug in the first version of the code (see text).

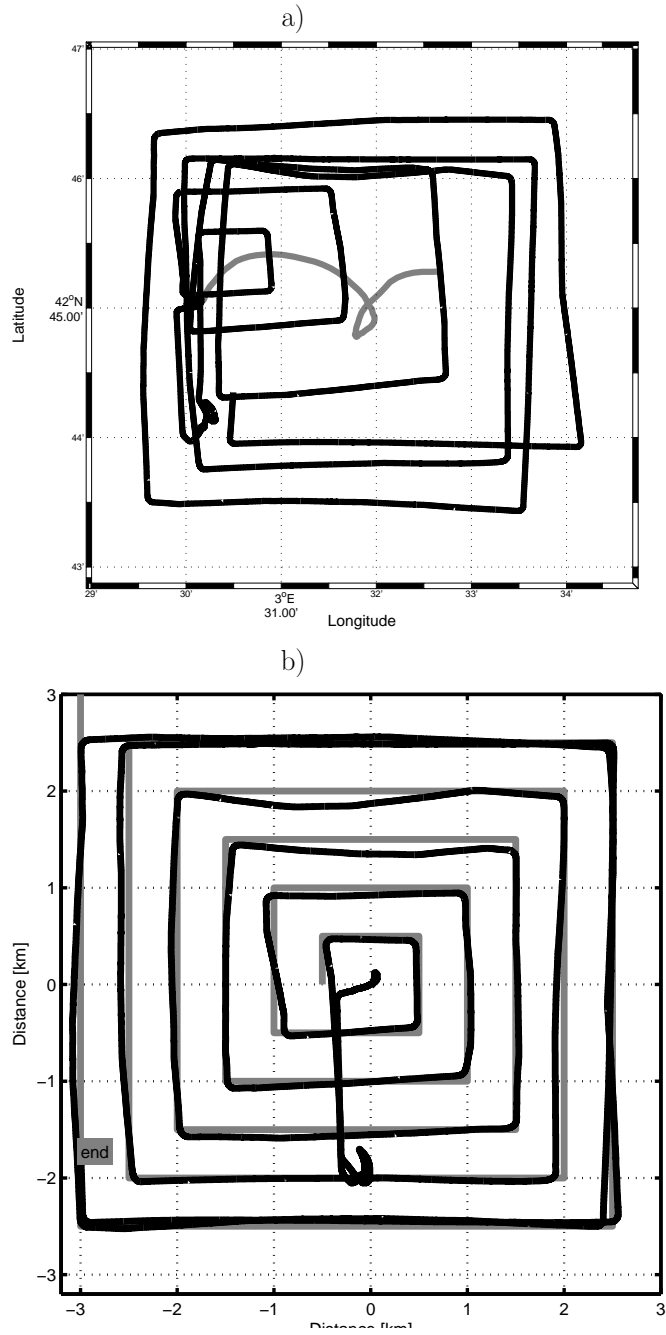


FIG. 6. Same as Fig. 2, but for the tracer release during the Latex10 cruise.